Theoretical and Experimental Results of High-Birefringent Fiber Loop Mirror With an Output Port Probe

Ricardo Manuel Silva, Azam Layeghi, Mohammad Ismail Zibaii, Hamid Latifi, Jose Luis Santos, *Member, OSA*, and Orlando Frazão, *Member, OSA*

(Invited Paper)

***Abstract*—Theoretical and experimental results of three different high-birefringent fiber loop mirrors with output ports are analyzed. For theoretical model, the Jones matrix analysis is used. The theoretical studies present similar results for all experimental configurations. The last configuration is tested as an interrogation system where the spectral response arises from the combination of the reference signal modulated by the sensor signal. The configuration is characterized in strain with the phase changes recovered from two quadrature phase signals, providing a sensitivity of 16 mrad/$\mu\varepsilon$ with a resolution of 1.9 $\mu\varepsilon$.**

***Index Terms*—High-birefringent fiber loop mirror (Hi-Bi FLM), interferometer, optical fiber sensor, strain.**

I. Introduction

SINCE the end of the 1980s, the fiber loop mirror (FLM) has been shown to be an attractive device for optical fiber sensing [1]. The loop mirror is made up of a splice between the output ports of one directional optical coupler. In this case, the two waves travel with identical optical paths in opposite directions and a constructive interference is assured when the waves reenter the coupler. Afterward, all light is reflected back into the input port, while no light is transmitted to the output port. The reflectivity is limited by the losses of the splice, fiber, and coupler. When a section of highly birefringent (Hi-Bi) fiber is spliced inside the FLM, a path imbalance is introduced as a consequence of propagation of light along different polarization eigenaxis, and thus, an interferometric channeled spectrum is observed. This configuration is an unbalanced Sagnac interferometer. The fiber birefringence and the fiber length inside the loop determine the channel separation of the pattern fringe [2]. Over the last decade, several high-birefringent fiber loop mirrors (Hi-Bi FLM) applications as sensors have been reported, through the inclusion of different types of Hi-Bi fibers [3]. Besides the gyroscope application [4], the Hi-Bi FLM has been used in temperature [2], [5] and strain [6] measurement, liquid level [7], displacement sensing [8], and refractometers [9], as well as a spectral filter for fiber Bragg grating demodulation [10]. Furthermore, the Hi-Bi FLM combined with other optical devices was also demonstrated for simultaneous measurement of strain and temperature [11]. Preliminary works using a Hi-Bi FLM with an output port probe were recently demonstrated [12]. These configurations presented similar sensitivities to strain when compared with the conventional Hi-Bi FLM. One of the configurations was used as refractometer using the Fresnel reflection [12].

In this paper, the authors present a theoretical model of three different Hi-Bi FLMs with an output port configuration. The last experimental setup is studied as a strain sensor using a reference signal to reconstruct the phase signal of the sensor.

II. Theoretical Analysis

Three configurations of Hi-Bi FLMs are schematically shown in Fig. 1. They consist of a loop of optical fiber formed between the output ports of two directional couplers along with an output port probe. The input light, constituted by one wave, travels from the optical source towards the first optical coupler (input port 1) and splits in two waves with half power, each traveling from output ports 3 and 4, following different optical paths. One arm of the FLM has a polarization controller (PC). The two waves couple into the second optical coupler for the output port 7 and reach the mirror. Afterward, they are reflected and arrive to the port 7, where the two waves are separated once more by the second optical coupler. Four waves are thus obtained at the output ports of the second coupler. Two waves are combined in the first coupler with opposite directions and the same optical path. Half of the light is then reflected back into the input port. This behavior is similar to the conventional Hi-Bi FLM [1]. The

Manuscript received May 30, 2011; revised August 31, 2011; accepted September 01, 2011. Date of publication September 22, 2011; date of current version March 02, 2012.

R. M. Silva and O. Frazão are with INESC Porto—Instituto de Engenharia de Sistemas e Computadores do Porto, 4169-007 Porto, Portugal (e-mail: rmsilva@inescporto.pt; ofrazao@inescporto.pt).

A. Layeghi was with Laser and Plasma Research Institute, Shahid Beheshti University, Tehran 1983963113, Iran. She is now with INESC Porto—Instituto de Engenharia de Sistemas e Computadores do Porto, 4169-007 Porto, Portugal (e-mail: a.layeghi@gmail.com).

M. I. Zibaii is with Laser and Plasma Research Institute, Shahid Beheshti University, Tehran 1983963113, Iran, and also with INESC Porto—Instituto de Engenharia de Sistemas e Computadores do Porto, 4169-007 Porto, Portugal (e-mail: mizibaye@gmail.com).

H. Latifi is with the Laser and Plasma Research Institute, Shahid Beheshti University, Tehran 1983963113, Iran (e-mail: latifi@cc.sbu.ac.ir).

J. L. Santos is with the Department of Physics and Astronomy, Faculty of Sciences, University of Porto, 4169-007 Porto, Portugal (e-mail: josantos@fc.up.pt).

Digital Object Identifier 10.1109/JLT.2011.2167499

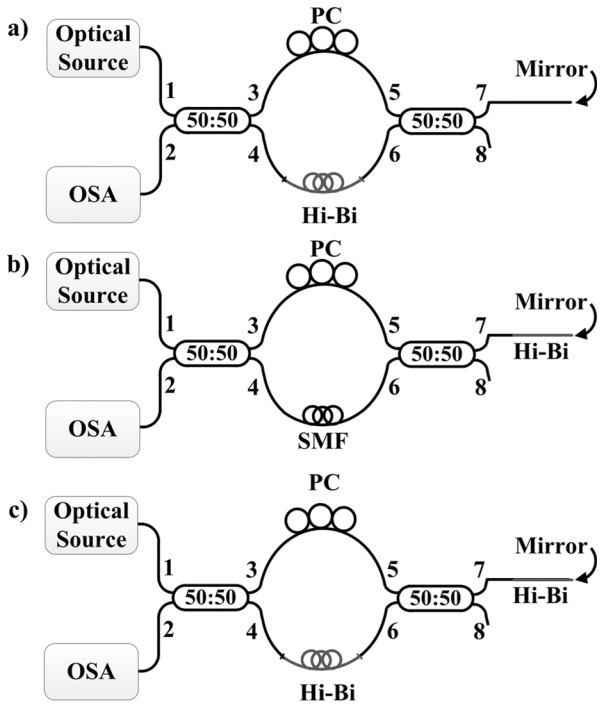

Fig. 1. Schematic setup for the (a) first, (b) second, and (c) third new Hi-Bi FLM configurations.

other two waves have a different optical path resulting into a channeled spectrum with a short periodicity not resolved by the optical spectrum analyzer (OSA), which reads only the averages powers of these waves. The difference between the three configurations was the localization of the Hi-Bi fiber section. In the first configuration [see Fig. 1(a)], it was placed between the two couplers, while in the second one [see Fig. 1(b)], in the output probe. The last configuration consisted on the combination of the first and second setups.

In this study, the Jones matrix analysis was used to calculate the transmission field. The Hi-Bi fiber section used in the first configuration [see Fig. 1(a)] had a length of 0.36 m. An equivalent optical circuit of the first configuration proposed is shown in Fig. 2(a). The Jones matrix analysis of the transmission field of the first configuration is expressed as

$$E_{\mathrm{OUT}} = \{[K_I][J_{\mathrm{HB}}][K_C] + [K_C][J_{\mathrm{PC}}][K_I]\} \times [J_M] \times \{[K_C][J_{\mathrm{HB}}][K_C] + [K_I][J_{\mathrm{PC}}][K_I]\} E_{\mathrm{in}} \quad (1)$$

with

$$[J_{\mathrm{HB}}] = \begin{bmatrix} e^{j\beta_e L} 0 \\ 0 e^{j\beta_o L} \end{bmatrix}, \quad [J_M] = \begin{bmatrix} 1 & 0 \\ 0 & -1 \end{bmatrix} \quad (2)$$

$$[J_{\mathrm{PC}}] = \begin{bmatrix} \cos\theta & -\sin\theta \\ \sin\theta & \cos\theta \end{bmatrix} \begin{bmatrix} e^{j\Gamma(\lambda)/2} & 0 \\ 0 & e^{j\Gamma(\lambda)/2} \end{bmatrix} \times \begin{bmatrix} \cos\theta & \sin\theta \\ -\sin\theta & \cos\theta \end{bmatrix} \quad (3)$$

where $[J_{\mathrm{HB}}]$, $[J_M]$, and $[J_{\mathrm{PC}}]$ are the Jones matrices of the Hi-Bi fiber, the mirror, and the PC, respectively. Here, the propagation constants along the e axis and o axis of the Hi-Bi fiber are represented by β_e and β_o, respectively, and the length of the Hi-Bi fiber is expressed as L. Based on the birefringence of the Hi-Bi fiber $B = (n_e - n_0)$, the difference between the propagation constants is $\beta_e - \beta_o = 2\pi B/\lambda$. Γ is the retardance and θ is the orientation of the wave plate axes with respect to the laboratory coordinates. The others matrices are given by

$$[K_I] = [K_{1,3}] = [K_{5,7}] = [K_{4,2}] = \begin{bmatrix} \sqrt{0.50} \\ 0\sqrt{0.5} \end{bmatrix} \quad (4)$$

$$[K_C] = [K_{1,4}] = [K_{6,7}] == [K_{3,2}] = \begin{bmatrix} j\sqrt{0.50} \\ 0j\sqrt{0.5} \end{bmatrix} \quad (5)$$

where $[K_1]$ and $[K_C]$ are the in-coupling and cross-coupling matrices, respectively, for the 3 dB optical coupler. The theoretical result of the first configuration is shown in Fig. 3(a) and is in concordance with the experimental results. At the second configuration, as shown in Fig. 1(b), the Hi-Bi fiber with the same length of the first configuration was laid in the output probe. There were 2 m of single-mode fiber (SMF) instead of Hi-Bi fiber, when comparing with the first configuration. The equivalent optical circuit of the second configuration is shown in Fig. 2(b), where the Jones matrix analysis is expressed as

$$E_{\mathrm{OUT}} = \{[K_I][J_{\mathrm{SMF}}][K_C] + [K_I][J_{\mathrm{PC}}][K_I]\} \times [J_{\mathrm{HB}}] \times [J_M] \times [J_{\mathrm{HB}}] \times \{[K_C][J_{\mathrm{SMF}}][K_C] + [K_I][J_{\mathrm{PC}}][K_I]\} E_{\mathrm{in}} \quad (6)$$

$$[J_{\mathrm{SMF}}] = \begin{bmatrix} 1 & 0 \\ 0 & 1 \end{bmatrix} e^{i\Delta\varphi} \quad \text{and} \quad \Delta\varphi = \frac{2\pi n \Delta L}{\lambda} \quad (7)$$

where n is the fiber core refractive index of the SMF and ΔL is the difference of fiber length between the two arms of the loop. The simulated Hi-Bi fiber effect in the second configuration is shown in Fig. 3(b). Similar theoretical and experimental results were obtained. The simulation results of the visibility variation using the PC in the second experimental setup are shown in Fig. 4.

In Fig. 2(c), an equivalent optical circuit is presented for the proposed FLM interferometer shown in Fig. 1(c). This configuration is practically the same as the second one, only $[J_{\mathrm{SMF}}]$ and $[J_{\mathrm{HB}}]$ are replaced with $[J_{\mathrm{HBR}}]$ and $[J_{\mathrm{HBS}}]$, respectively. The HB_R and HB_S correspond to the reference and sensor Hi-Bi fibers, respectively. The transmission spectra simulation results are shown in Fig. 5(a) for the sensor without the reference signal. Fig. 5(b) exhibits the spectral response for the sensor combined with the reference signal. Comparing the two first results, the theoretical model is in good agreement with the two experimental results obtained. The last configuration presents some discrepancy due to the experimental setup is not optimized with a polarization control in the second Hi-Bi fiber section.

III. Experimental Details

The last configuration [see Fig. 1(c)] was characterized as an interrogation setup for strain measurement. In this case, two Hi-Bi fiber sections were used as sensor and reference. An optical broadband source with a bandwidth of 100 nm and a central wavelength of 1570 nm was used. The setup was formed by two simple couplers with low insertion loss, where the two output ports of the first coupler were spliced to the two input ports of the second one. In one of the splices, a Hi-Bi fiber section (reference) was inserted, while in the other arm a PC was placed, in

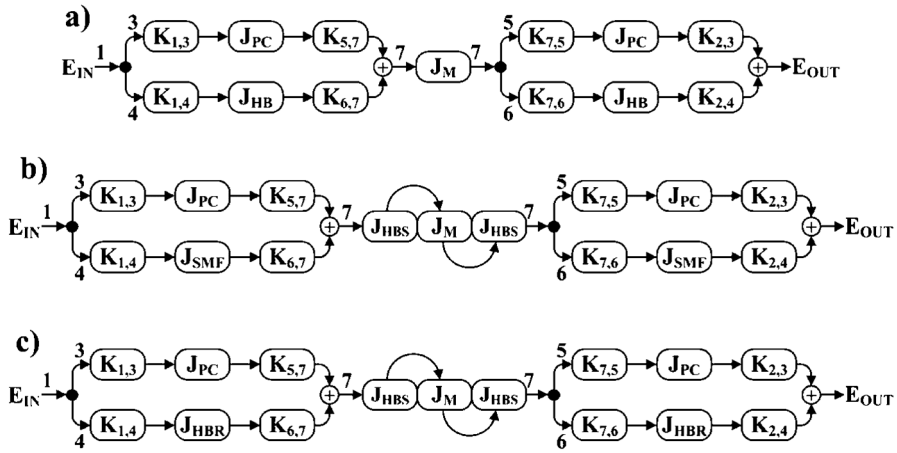

Fig. 2. Equivalent optical circuit of the proposed three configurations: (a) first, (b) second, and (c) third new Hi-Bi FLM configurations.

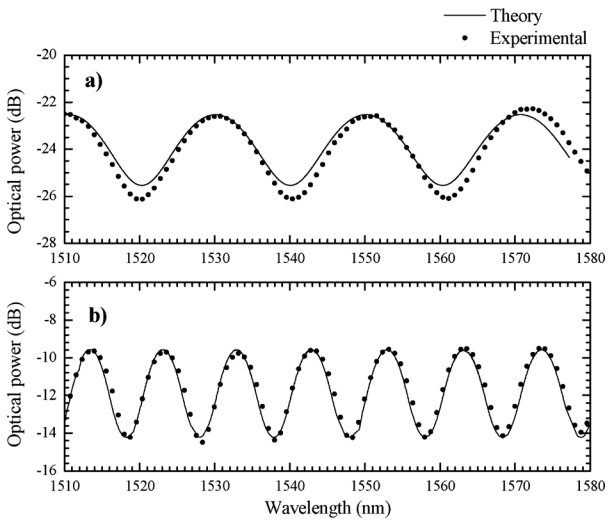

Fig. 3. Simulation and experimental results of the spectral response for the (a) first and (b) second configurations.

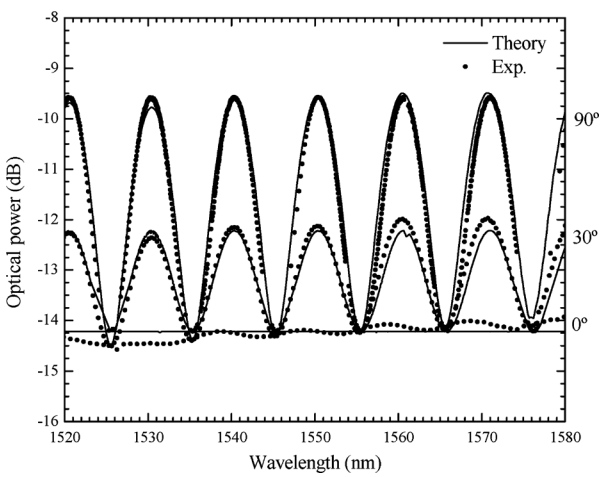

Fig. 4. Simulation and experimental results of the interferometric visibility variation of the second configuration using only a PC.

order to optimize the spectral response of the fringe pattern. The sensor was located at the output port of the second coupler and consists of the same type of Hi-Bi fiber. With the insertion of

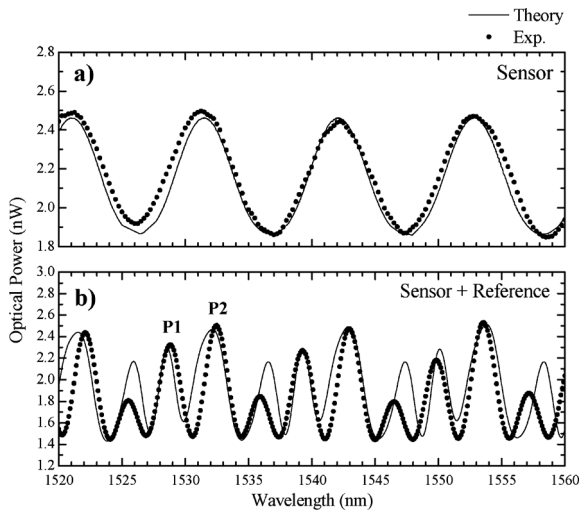

Fig. 5. Simulation and experimental result of spectral response of (a) sensor and (b) signals combined (sensor + reference).

two Hi-Bi fiber sections, the configuration will have two combined unbalanced Sagnac interferometers. The Hi-Bi fiber used was a PANDA fiber (PM-1550-HP) with a length of 1.34 m and 0.34 m for the reference and sensor signal, respectively. All results were monitored using an OSA with a maximum resolution of 0.05 nm. The LabVIEW software was used to process the data acquired through the OSA. A real-time signal processing was applied based on the generation of interferometric quadrature signals from the reference. The glue used to fix the fiber sensor was cyanoacrylate adhesive and its properties remained the same over the range of the applied physical parameters that were considered.

Fig. 5(a) shows the transmission spectrum of the sensor, which was obtained without the reference signal included in the experimental setup. The sensor wavelength periodicity was $\sim$11.2 nm, corresponding to a group birefringence of 3.3×10^{-4}. Fig. 5(b) shows a fringe pattern for the sensor signal combined with the reference signal. Two different frequencies were observed. The higher frequency corresponds to the reference signal and has a wavelength periodicity of $\sim$4 nm. The lower frequency, shown from the amplitude modulation of the reference signal, was due

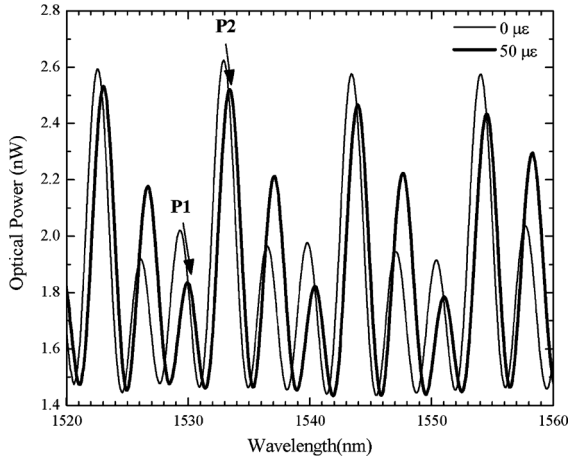

Fig. 6. Spectral response when the sensing head is subjected to strain.

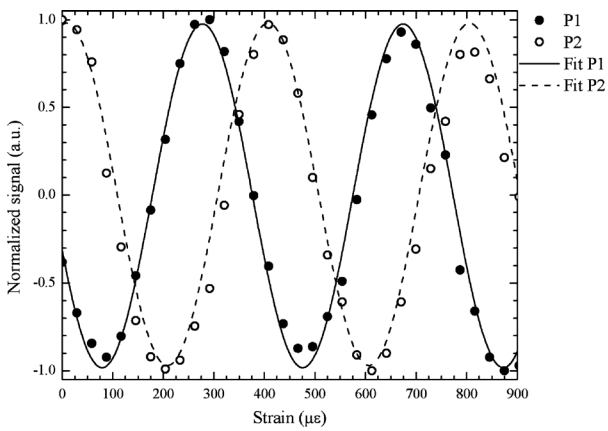

Fig. 7. Normalized output signals versus the strain, and the respective fits made to the experimental data.

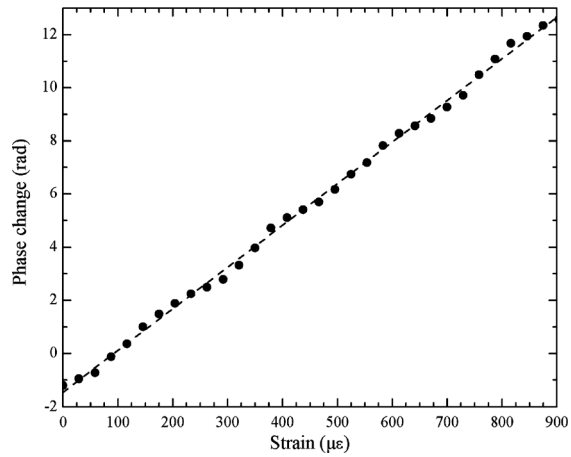

Fig. 8. Relationship between the phase signal change and the strain variation.

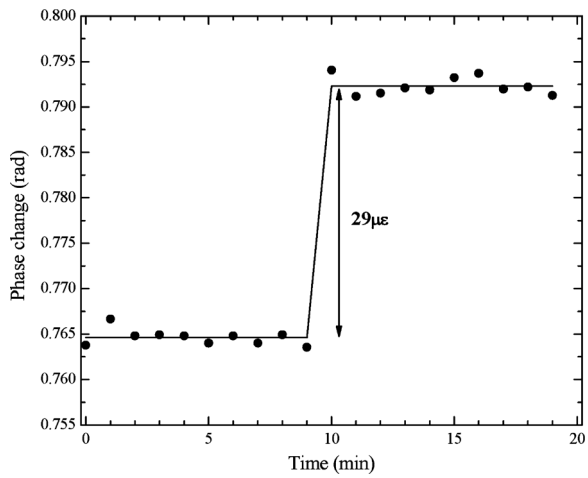

Fig. 9. Strain sensor resolution of sensing head.

to the sensor response. For strain characterization, the sensing head was attached to a translation stage with a resolution of 1 μm. Fig. 6 shows the response of the sensor when it was unstrained and when it was subjected to 50 $\mu\varepsilon$. An amplitude variation of the reference signal can be observed due to the fringe pattern wavelength shift of the sensor when strain was applied. Peaks P_1 and P_2 evidenced in the figure were in quadrature and their spectral variation is a consequence of the strain induced optical path difference change in the Hi-Bi sensing section when strain was applied. Using the two peaks variation, it was possible to reconstruct the pattern fringe of the sensor signal. In this case, the two peaks in quadrature were enough to measure the phase variation of the sensor. The normalized amplitude outputs represented in Fig. 7 were obtained from both peaks. Besides the amplitude variation of the peaks when strain was applied, their fits are also represented. A quadrature phase-shifted relation can be observed between these two signals, which allows the phase recovery from

$$\phi = \tan^{-1}\left(\frac{P_{1\mathrm{n}}}{P_{2n}}\right) \tag{8}$$

where $P_{1\mathrm{n}}$ and $P_{2\mathrm{n}}$ are the normalized optical powers of P_1 and P_2, respectively [13]. The strain induced phase change is shown in Fig. 8. Strain was applied between 0 and 900 $\mu\varepsilon$, resulting in a linear slope with a sensitivity of 16 mrad/$\mu\varepsilon$. Fig. 9 illustrates the system response for a strain step variation of 29 $\mu\varepsilon$. From the phase step change and noise level, it turns out a system resolution of 1.9 $\mu\varepsilon$.

IV. Conclusion

A theoretical analysis based on Jones matrix formalism addressing three new FLM configurations was performed. The results obtained confirm that the three setups presented a behavior of an FLM. The first configuration, where the Hi-Bi section was spliced between the two couplers, can be used as reference setup to interrogate other interferometric sensors. The second setup can be used to interrogate different Hi-Bi fiber sections subjected to different physical or chemical interactions. The last configuration was experimentally analyzed in this paper when applied to strain measurement. It was observed that with the two Hi-Bi fiber sections in the FLM, the spectrum of the reference signal was modulated by the sensing head spectral response. The amplitude variation of the reference signal was due to the change on fringe pattern wavelength of the sensing head. The phase change of the sensing head was monitored through the two peaks power response in quadrature phase shift of the reference signal, resulting into values for the sensitivity and resolution of 16 mrad/$\mu\varepsilon$ and 1.9 $\mu\varepsilon$, respectively. Comparing with a traditional Hi-Bi FLM,

this setup provides the elimination of the phase fluctuations that can occur between the sensor and reference signals, increasing its potential for remote sensing applications.

REFERENCES

[1] D. Mortimore, "Fiber loop reflectors," *J. Lightw. Technol.*, vol. 6, no. 7, pp. 1217–1224, Jul. 1988.

[2] A. N. Starodumov, L. A. Zenteno, D. Monzon, and E. De La Rosa, "Fiber Sagnac interferometer temperature sensor," *Appl. Phys. Lett.*, vol. 70, no. 1, pp. 19–21, 1997.

[3] O. Frazão, J. M. Baptista, and J. L. Santos, "Recent advances in high-birefringence fiber loop mirror sensors," *Sensors*, vol. 7, pp. 2970–2983, 2007.

[4] B. Culshaw, "The optical fibre Sagnac interferometer: An overview of its principles and applications," *Meas. Sci. Technol.*, vol. 17, pp. R1–R16, 2006.

[5] E. De la Rosa, L. A. Zenteno, A. N. Starodumov, and D. Monzon, "All-fiber absolute temperature sensor using an unbalanced high-birefringence Sagnac loop," *Opt. Lett.*, vol. 22, pp. 481–483, 1997.

[6] M. Campbell, G. Zheng, A. S. Holmes-Smith, and P. A. A. Wallace, "Frequency-modulated continuous wave birefringent fiber-optic strain sensor based on a Sagnac ring configuration," *Meas. Sci. Technol.*, vol. 10, pp. 218–224, 1999.

[7] D. Bo, Z. Qida, L. Feng, G. Tuan, X. Lifang, L. Shuhong, and G. Hong, "Liquid-level sensor with a high-birefringence-fiber loop mirror," *Appl. Opt.*, vol. 45, no. 30, pp. 7767–7771, 2006.

[8] Y. Liu, B. Liu, X. Feng, W. Zhang, G. Zhou, S. Yuan, G. Kai, and X. Dong, "High-birefringence fiber loop mirrors and their applications as sensors," *Appl. Opt.*, vol. 44, no. 22, pp. 2382–2390, 2005.

[9] O. Frazão, B. V. Marques, P. Jorge, J. M. Baptista, and J. L. Santos, "High birefringence D-type fibre loop mirror used as refractometer," *Sens. Actuators B-Chem*, vol. 135, pp. 108–111, 2008.

[10] S. Chung, J. Kim, B.-A. Yu, and B. Lee, "A fiber Bragg grating sensor demodulation technique using a polarization maintaining fiber loop mirror," *IEEE Photon. Technol. Lett.*, vol. 13, no. 12, pp. 1343–1346, Dec. 2001.

[11] O. Frazão, L. M. Marques, S. Santos, J. M. Baptista, and J. L. Santos, "Simultaneous measurement for strain and temperature based on a long period grating combined with a high-birefringence fiber loop mirror," *IEEE Photon. Technol. Lett.*, vol. 18, no. 22, pp. 2407–2409, Nov. 2006.

[12] O. Frazão, R. M. Silva, and J. L. Santos, "High-birefringent fiber loop mirror sensors with an output port probe," *IEEE Photon. Technol. Lett.*, vol. 23, no. 2, pp. 103–105, Jan. 2011.

[13] M. Dahlem, J. L. Santos, L. A. Ferreira, and F. M. Araújo, "Passive interrogation of low-finesse Fabry-Pérot cavities using fiber Bragg gratings," *IEEE Photon. Technol. Lett.*, vol. 13, no. 9, pp. 990–992, Sep. 2006.

Ricardo Manuel Silva received the M.Sc. degree in physics engineering from University of Aveiro, Aveiro, Portugal, in 2009.

He is currently a Researcher at Optoelectronics and Electronic Systems Unit, INESC Porto, Porto, Portugal. His research interest includes development of fiber-optic sensors.

Azam Layeghi received the M.Sc. degree in photonics from Laser and Plasma Research Institute, Shahid Beheshti University, Tehran, Iran, in 2007.

She was involved in the simulation of optical fiber laser. She is currently a Researcher at INESC Porto, Porto, Portugal. Her research interests include the simulation of fiber-optic sensors.

Mohammad Ismail Zibaii received the M.Sc. degree in photonics from Laser and Plasma Research Institute, Shahid Beheshti University, Tehran, Iran in 2005, where he is currently working toward the Ph.D. degree in photonics.

He is also a Ph.D. Student Researcher at INESC Porto, Porto, Portugal. His research interest includes development of fiber-optic sensors and label-free fiber-optic biosensors for DNA-Drug interaction, Bactria, and protein in low concentration.

Hamid Latifi received the B.S. degree from California state university in Harvard, and the M.Sc. and Ph.D. degrees from New-Mexico State University, Las Cruces, in 1989, all in physics, working on interaction of high-energy laser beam aerosols.

He was a Postdoctoral Research at Colorado State University in Fort Collins, working on development of sodium Lidar for mesospheric temperature measurement. He joined the Physics Faculty of Shahid Beheshti University (former: National University), Tehran, Iran, in 1991, where he is currently a Professor of physics at Laser and Plasma Research Institute. His current interest includes diode pumped solid state laser, RF-excited CO_2 lasers, optical nondestructive testing, and fiber-optic sensors.

Jose Luis Santos received the Graduate and Ph.D. degrees in physics from the University of Porto, Porto, Portugal, in 1983 and 1993, respectively. His Ph.D. degree was focused on research in fiber-optic sensing.

He is currently a Professor in the Department of Physics and Astronomy, Faculty of Sciences, University of Porto.

Dr. Santos is a member of the Optical Society of America and the International Society for Optical Engineers.

Orlando Frazão received the Degree in physics engineering (in optoelectronics and electronics) from the University of Aveiro, Aveiro, Portugal, and the Ph.D. degree in physics from the University of Porto, Porto, Portugal, in 2009.

From 1997 to 1998, he was with the Institute of Telecommunications, Aveiro. He is currently a Researcher at Optoelectronics and Electronic Systems Unit, INESC Porto, Porto, Portugal. He has published about 250 papers, mainly in international journals and conference proceedings. His current research interests include optical fiber sensors and optical communications.

Dr. Frazão is a member of the Optical Society of America and the International Society for Optical Engineers.